Research article

JGS
*Journal of the Geological Society*

Published online June 18, 2020 https://doi.org/10.1144/jgs2020-009 | Vol. 177 | 2020 | pp. 955–964

# The Paleogene ophiolite conundrum of the Iran–Iraq border region

**Hadi Shafaii Moghadam[1,2,3]*, Qiu-Li Li[3], Robert J. Stern[4], Massimo Chiaradia[5], Orhan Karsli[6] and Bahman Rahimzadeh[7]**

[1] School of Earth Sciences, Damghan University, Damghan 36716-41167, Iran
[2] FB4-Dynamics of the Ocean Floor, GEOMAR, Helmholtz-Zentrum für Ozeanforschung Kiel, Wischhofstr. 1-3, 24148 Kiel, Germany
[3] State Key Laboratory of Lithospheric Evolution, Institute of Geology and Geophysics, Chinese Academy of Geosciences, Beijing 100029, China
[4] Geosciences Department University of Texas at Dallas, TX 75083-0688, USA
[5] Department of Earth Sciences, University of Geneva, Geneva, Switzerland
[6] Department of Geological Engineering, Recep Tayyip Erdoğan University, Rize TR-53100, Turkey
[7] Faculty of Earth Sciences, Shahid Beheshti University, Tehran, Iran
HSM, 0000-0002-3674-9764; Q-LL, 0000-0002-7280-5508; RJS, 0000-0002-8083-4632; MC, 0000-0003-4943-2480
* Correspondence: hshafaei@geomar.de

**Abstract:** New and compiled geochemical, isotopic and geochronological data allow us to propose a new explanation for Paleogene oceanic magmatic rocks along the Iran–Iraq border. These rocks are represented by a thick pile (>1000 m) of pillow lavas and pelagic sediments and underlying plutonic rocks. These are sometimes argued to represent a Paleogene ophiolite but there are no associated mantle rocks. Integrated zircon U–Pb ages, bulk rock major and trace element and radiogenic isotope data indicate that these rocks are more likely related to forearc rifting due to extreme extension during Late Paleogene time which also triggered high-flux magmatism in the Urumieh–Dokhtar Magmatic Belt and exhumation of core complexes in Iran. These observations are most consistent with formation of the Paleogene oceanic igneous rocks in a >220 km long forearc rift zone.

Supplementary material: Detailed analytical procedure and tables S1 to S6 are available at: https://doi.org/10.6084/m9.figshare.c.4972994

**Received** 14 January 2020; **revised** 16 April 2020; **accepted** 11 May 2020

Iran and Iraq contain many ophiolites of Mesozoic (mostly Late Cretaceous) age (Moghadam and Stern 2015). Late Cretaceous ophiolites are especially abundant along the Zagros suture zone of Iran and Iraq. Geochronological and geochemical data from Zagros ophiolites strongly support Neotethyan subduction initiation (SI) beneath SW Eurasia during earliest Late Cretaceous and maturation of the convergent margin in latest Cretaceous and Paleogene time (e.g. Golonka 2004; Moghadam and Stern 2011; Moghadam and Stern 2015; Nouri *et al.* 2016; Monsef *et al.* 2018). Subduction initiation was coincident with equivalent ophiolites in Oman and the eastern Mediterranean area (Cyprus, Turkey, Syria to Iraq) (Dilek *et al.* 2007; Dilek and Thy 2009; Moghadam and Stern 2011; van Hinsbergen *et al.* 2019). Late Cretaceous ophiolites are intruded and covered by younger, Cenozoic intrusions and volcano-sedimentary rocks. Abundant Cenozoic igneous rocks in Iran are readily distinguished because they tend to be felsic and eruptions were subaerial or in shallow water. However, along the Iran–Iraq border Cenozoic igneous rocks are often mafic and submarine and are easily confused with Late Cretaceous ophiolites (Fig. 1a, b). The presence of gabbros and overlying pillow lavas has led to these being described as a Paleogene ophiolite (e.g. Ao *et al.* 2016). Do Paleogene mafic-submarine mafic igneous rocks along the Iran–Iraq border really represent oceanic crust? Crucially, what is their significance in the framework of Neotethyan ophiolite and SW Eurasian tectonic evolution?

There are several interpretations for the genesis of these rocks. For example, Saccani *et al.* (2014) described these rocks as Permian–Triassic passive margin-type ophiolite related to the Gondwana rifting and Neotethyan opening. Paleocene–Oligocene arc to back-arc basin models are also used to explain the occurrence of these rocks along the Zagros suture zone (Azizi *et al.* 2011; Ali *et al.* 2013). A complex model involving Paleocene back-arc rifting and Eocene arc construction within the Paleocene back-arc basin along the Eurasian continental margin is also used to explain the occurrence of these rocks (Whitechurch *et al.* 2013). Ao *et al.* (2016) argued that the Paleogene oceanic realm reflected an exhumed Eocene oceanic core complex, which triggered remelting of oceanic gabbros to make Paleogene granites. Another model considers slab breakoff – following Early Paleogene continental collision – and development of a slab window, which facilitated partial melting of metasomatized lithospheric mantle to make Paleogene igneous rocks along the Iran–Anatolia margin (Dilek and Altunkaynak 2010). This controversy is usefully referred to as the 'Paleogene ophiolite conundrum'.

In this paper, we report new data on Paleogene magmatic assemblages near Kermanshah-Kamyaran, Iran, near the Iran–Iraq border region. We report new whole rock major and trace element and whole rock Sr–Nd–Pb isotope data along with zircon U–Pb ages and O–Hf isotopes and use these to better understand the age, geochemical signatures and source of these rocks. We further integrate our new data with published results to resolve the 'Paleogene ophiolite conundrum' and identify for the first time an important Eocene oceanic rift zone that developed along the present border of Iran and Iraq with possible continuation into easternmost Turkey (Fig. 1b).

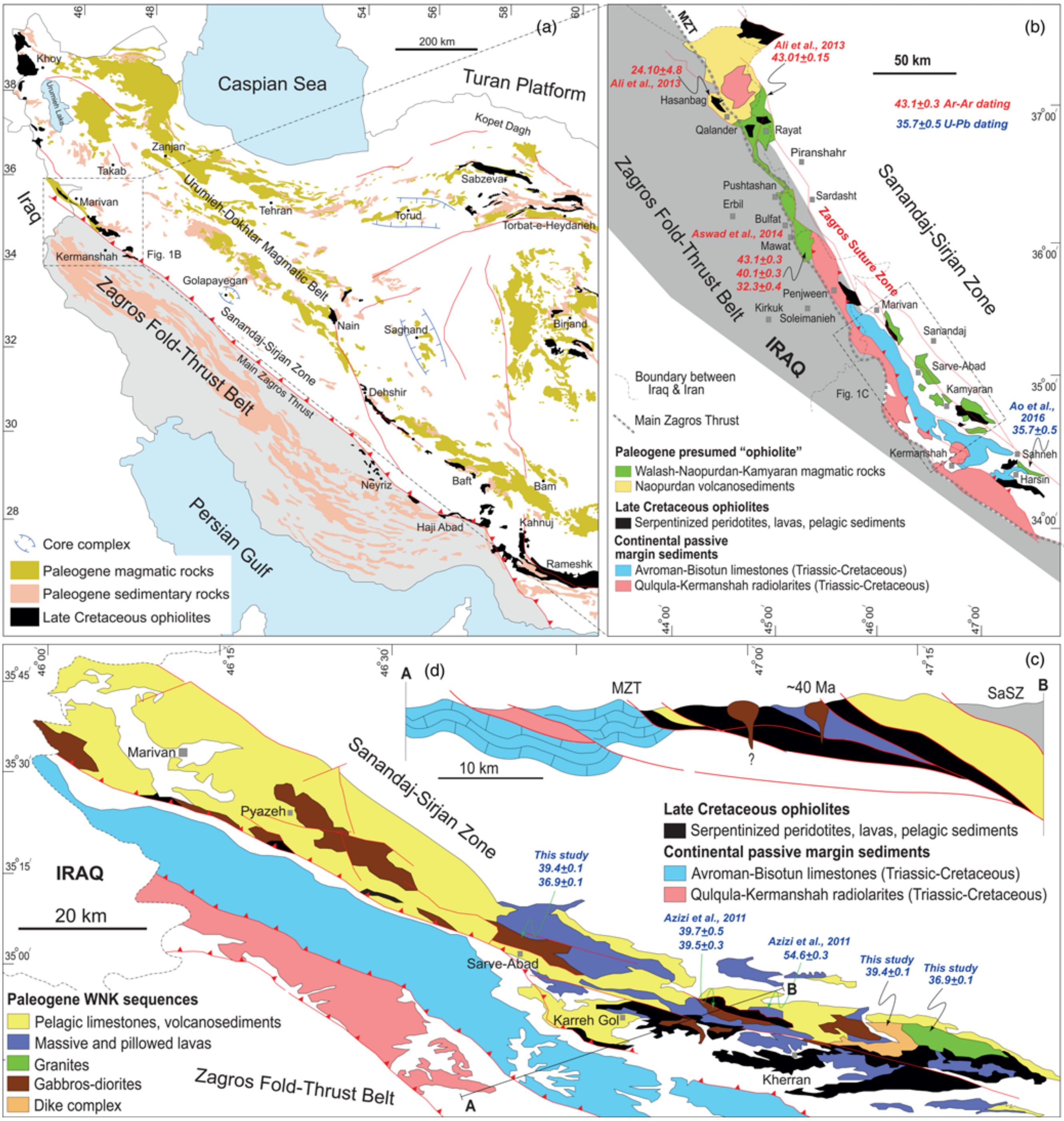


**Fig. 1.** (**a**) Geological map of Iran and environs showing Paleogene magmatic and sedimentary rocks and Late Cretaceous ophiolites. (**b**) Simplified map showing the distribution of Late Cretaceous forearc ophiolites and Paleogene oceanic rocks (Walash–Naopurdan–Kamyran series) along the Iran–Iraq border (modified after Ali *et al.* (2013)). Numbers refer to ages in Ma. (**c**) Geological map of Paleogene magmatic and sedimentary sequences along the Iran–Iraq border showing the location of dated samples. Numbers refer to ages in Ma. A–B line shows the cross-section position in Figure 1d. (**d**) Schematic cross section showing the relations between the Paleogene intrusions and older lithological units (modified after Agard *et al.* (2005)).

## Late Cretaceous forearc ophiolites of the Iran–Iraq border region

Late Cretaceous SI-related Zagros ophiolites are present in the Kurdistan region of eastern Iraq and western Iran, around Kermanshah and Sahneh–Harsin (Fig. 1b). These ophiolites continue to the SE towards Neyriz and Haji-Abad ophiolites (Fig. 1a). Ophiolites in the Kurdistan region are associated with thick Triassic–Cretaceous sequence of pelagic limestones (Avroman–Bisotun limestones), radiolarites (Qulqula–Kermanshah radiolarites) and ocean island basalt (OIB)-, incompatible element-enriched (E-) mid-ocean ridge basalt (MORB)-like lavas and minor felsic intrusive and extrusive rocks which are similar to Triassic (*c.* 230 Ma) alkaline magmatism of the Hawasina Nappes of Oman (Chauvet *et al.* 2011). These units are found near the Main Zagros Thrust (MZT; Fig. 1b, c) and are highly crushed. The along-strike continuation of these units to the SE is known as the Pichakun series in Neyriz, which consist of upper Triassic limestones, middle Jurassic oolitic limestones and lower-middle Cretaceous conglomeratic limestones. Minor OIB-like lavas accompany these sediments (Babaei *et al.* 2005).

These sequences are related to rifting of Gondwana and opening of Neotethys. These units continue into Iraqi Kurdistan (Mawat to Hasanbag, Fig. 1b) where they are known as the Avroman limestones and Qulqula radiolarites.

The Late Cretaceous forearc ophiolite around Kermanshah includes mantle peridotite, gabbro, minor plagiogranite, Nb–Ta depleted arc tholeiitic to calc-alkaline lava and Turonian–Maastrichtian pelagic limestone. Gabbroic dikes within the Kermanshah ophiolite mantle section are dated at *c.* 97 Ma and Kermanshah plagiogranites have zircon U–Pb ages of 94.6 ± 2.7 to 99.5 ± 0.2 Ma (Nouri *et al.* 2016). Further to the SE, in Neyriz and Haj-Abad, Late Cretaceous ophiolites include depleted to highly impregnated harzburgites containing screens of residual dunite, chromitite, pyroxenitic sills/dikes, pegmatite gabbros and diabasic–basaltic–andesitic dikes. Sheeted dikes and pillow lavas construct the crustal sequence of these ophiolites. $^{40}Ar/^{39}Ar$ age data from crustal plagiogranites yield ages of 92.07 ± 1.69 and 93.19 ± 2.48 Ma (Babaie *et al.* 2006), whereas zircon U–Pb data show ages of 100.1 ± 2.3 to 93.4 ± 1.3 Ma (Monsef *et al.* 2018).

Zagros ophiolites show strong supra-subduction zone geochemical signatures, both for mantle and crustal rocks (Ghazi *et al.* 2010; Moghadam *et al.* 2010; Moghadam and Stern 2011; Monsef *et al.* 2018). The crustal sequence of Zagros ophiolites is represented by MORB-like lavas similar to forearc basalts (FAB), arc tholeiites and boninites, similar to present-day forearcs (Ishizuka *et al.* 2014), although Zagros igneous rocks have stronger Nb–Ta depletion, variable mantle sources and contributions of various subduction components during their genesis (Moghadam *et al.* 2012, 2013*b*, 2014). Magmatic rocks with boninitic compositions (Ti/V < 10 and a depleted REE pattern) occur in the Haj-Abad (egg-shaped pillow lavas), Neyriz (sheeted dike complex) and Kermanshah (massive lava) (Moghadam and Stern 2011; Moghadam *et al.* 2013*a*). Zagros MORB-like rocks both pre-date and post-date boninites. The Zagros system, like other intra-oceanic forearcs, finally erupted calc-alkaline felsic lavas with Ti/V > 10 and high V/Sc.

## Paleogene oceanic tracts of the Iran–Iraq border region

Paleogene volcano-sedimentary rocks are abundant for > 220 km long on either side of the Iran–Iraq border, from SE of Kermanshah to Hasanbag (Fig. 1b). These rocks are called the Walash and Naopurdan volcano-sedimentary sequences in Iraq; we informally call them the Kamyran series here. Paleogene rocks also occur as bimodal intrusive rocks (*c.* 41 Ma alkaline gabbros and $A_2$-type granites) in northwestern parts of Piranshahr (Mazhari *et al.* 2009) (Fig. 1b). The Walash–Naopurdan–Kamyran (WNK) volcano-sedimentary rocks – along with intrusive rocks from NW Iran – are the western extension of the Urumieh–Dokhtar Magmatic Belt (UDMB), which represents the Paleogene magmatic arc of Iran to the east (Fig. 1a). These sequences are intruded by Paleogene granitoids and gabbros. The Walash and Naopurdan sequences consist of pillow and massive basalts, andesites and pyroclastic rocks associated with sandstones, limestones and cherts. The thickness of the Walash–Naopurdan series varies up to > 3000 m. These rocks are mixed and fault-bounded with Late Cretaceous Iraqi ophiolites and even Permian–Triassic OIB-type lavas and limestones (Ali *et al.* 2013; Hassan *et al.* 2015). Recent $^{40}Ar/^{39}Ar$ radiometric dating on basaltic–andesitic feldspars and whole rocks near Hasanbag indicates ages of *c.* 43–24 Ma; 43.01 ± 0.15 on Walash and 34.33 ± 0.91to 24.10 ± 4.8 Ma on Naopurdan rocks (Ali *et al.* 2013). In the Mawat area, $^{40}Ar/^{39}Ar$ geochronological data indicate that Walash andesites erupted at 43.1 ± 0.3, 40.1 ± 0.3 and 32.3 ± 0.4 Ma (Aswad *et al.* 2014). Igneous rocks of the Walash and Naopurdan series have subduction-related characteristics, and include both arc tholeiites and calc-alkaline rocks (Aswad 1999; Numan 2001; Aswad *et al.* 2011; Aziz *et al.* 2011*a*, *b*; Ali *et al.* 2013). These geochemical characteristics are similar to those of Eocene arc-related volcano-sedimentary rocks from Kamyaran (Azizi *et al.* 2011). The formation of the Walash and Naopurdan volcano-sedimentary series has been ascribed to an intra-oceanic convergent margin and development of an arc-back-arc setting during Paleocene–Oligocene (and even Miocene) time (Ali *et al.* 2013). Eocene volcano-sedimentary rocks are similarly present along the Bitlis–Zagros suture zone in SE Turkey, where their genesis is ascribed to Neotethys subduction, slab detachment, extension and melting of a sub-continental lithospheric mantle (Dilek *et al.* 2010).

The Paleogene intrusive rocks also occur around Kamyaran and are dominant at SE of Kermanshah, in Sahneh and Harsin. Around Kamyaran, these rocks intrude both Late Cretaceous ophiolitic rocks – especially serpentinites and harzburgites – and Paleogene volcano-sediments and lavas (Fig. 1c, d). Rocks from SE of Kermanshah include gabbros, granitoids and pillow lavas with arc tholeiitic signature and high εNd(t) values (+ 3.7 to + 9.8) (Nouri *et al.* 2017). Granites show a zircon U–Pb age of 35.7 ± 0.5 Ma (Ao *et al.* 2016). Granites and gabbros from Sahneh–Harsin intruded into Late Cretaceous harzburgites and Eocene volcano-sediments (Whitechurch *et al.* 2013). Azizi *et al.* (2011) also described a series of calc-alkaline to arc tholeiitic pillow basalts (Fig. 2a) and gabbros SE of Kamyaran, with zircon U–Pb ages of 54.6 ± 0.3 Ma and 36.75 ± 0.51 to 36.63 ± 0.40 Ma respectively. Initial εNd of these rocks is high (+ 2.8 to + 10), similar to those of intra-oceanic arcs (Azizi *et al.* 2011). There is also an (basaltic-)andesitic to dacitic dike complex that is intruded by granitic lenses (Fig. 2b). Paleogene dikes intruded Late Cretaceous Kermanshah ophiolites and Paleogene lavas cover them. We sampled dikes as well as lavas for geochemical-isotopic analysis and granitic-dacitic dikes for zircon U–Pb dating.

Paleogene oceanic sequences are also present NW of Kamyaran (east of Sarve Abad, Fig. 1b, c). This Paleogene sequence includes gabbros, diorites and granitic dikes at the lower parts with thickness of *c.* 3–4 km (Fig. 2c–e). The lower gabbroic–dioritic sequence grades into a thick pile (> 1000 m) of pillow lavas (Fig. 2f, g). The abundance of granitic dikes increases towards the contact of the intrusive rocks with pillow lavas. Gabbros and granites show intrusive contacts with both Paleogene volcano-sediments–sandstones and with thin slices of Late Cretaceous serpentinized harzburgites. To the WSW, this Paleogene sequence shows faulted contacts with Kermanshah radiolarites whereas in the ENE it has faulted contacts with Mesozoic rocks of the Sanandaj–Sirjan zone.

## Analytical procedures

We used five analytical techniques, including: (1) Cameca 1280-HR SIMS and (2) LA-ICPMS to analyse zircons for U–Pb ages and O isotopes; (3) Multicollector-inductively coupled plasma-mass spectrometer (MC-LA-ICPMS) for analysing Lu–Hf isotope composition of dated zircons; (4) X-ray florescence (XRF) and ICP-MS methods to analyse whole rock major and trace elements; and (5) Thermo Neptune PLUS Multi-Collector ICP-MS to analyse whole rock Sr, Nd and Pb isotopes. Detailed analytical procedures can be found in the Supplementary material.

## Zircon U–Pb geochronology and O–Hf isotopes

We analysed four samples of Paleogene igneous rocks from near Kamyran. Gabbros (sample KN14-14, from the lower part of the section) and granitic dike (sample KN14-3 which intrudes gabbros) from NW of Kamyaran (east of Sarve Abad, Fig. 1c) have intercept ages of 39.5 ± 0.3 Ma (Fig. 3a) and 39.7 ± 0.5 Ma (Fig. 3b), respectively. Two samples of SE Kamyaran dacitic dikes and

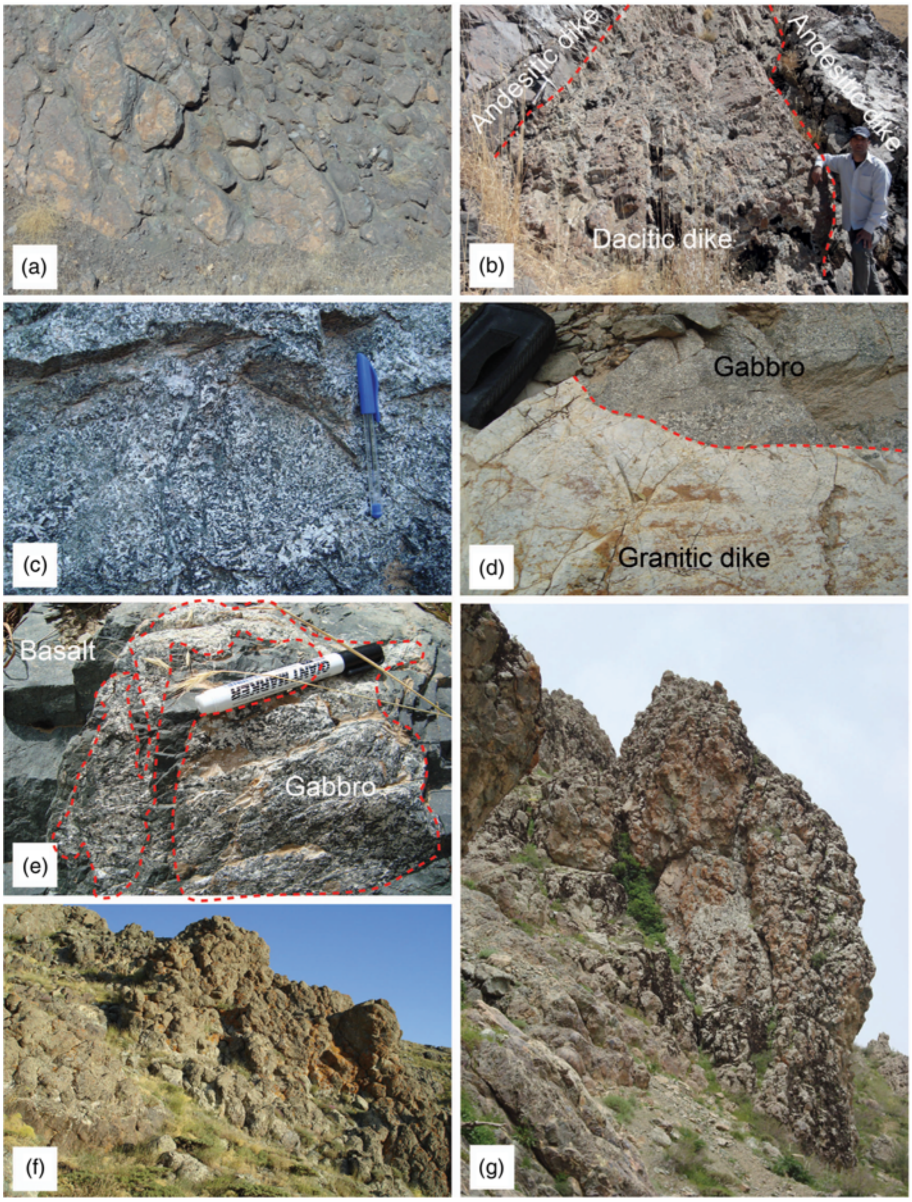


**Fig. 2.** (**a**) Outcrop of Paleogene pillow lavas from SE Kamyaran. (**b**) Contact between dacitic dikes and (basaltic-) andesitic dikes from SE Kamyaran. (**c**) Paleogene gabbros in NW Kamyaran. (**d**) Granitic dikes injected into gabbros. (**e**) Gabbro inclusions within the overlying pillow lavas – at the contact between gabbros and pillow lavas. (**f**) and (**g**) Outcrops of NW Kamyaran pillow lavas.

granites (cross-cutting dikes) have concordia ages of 36.9 ± 0.1 Ma (Fig. 3c) and 39.4 ± 0.1 Ma (Fig. 3d), respectively. These are related magmatic pulses that generated a significant igneous crust in a very short time.

The εHf(t) values for NW Kamyaran granitic zircons range from + 10.5 to + 16.3, whereas gabbro zircons have overlapping and slightly higher εHf(t) values of + 12.4 to + 18.8. The $\delta^{18}O$ values vary from + 5.3 to + 7‰ for granitic dike zircons and to overlapping and slightly lower values from + 4.9 to + 5.7‰ for gabbro zircons. The εHf(t) values for SE Kamyaran rocks varies from − 0.8 to − 7.6, indicating an unradiogenic source for these magmas, perhaps reflecting involvement of Cadomian continental crust.

## Whole rock major and trace elements and Sr–Nd–Pb isotopes

We analysed Paleogene gabbros, pillow lavas and granitic dikes from NW Kamyaran and dikes (from a dike complex) and lavas from SE Kamyaran. These are equivalent to the Walash–Naopurdan series of Iraq and the Kamyran series of Iran. Pillow lavas have slight light rare earth element (LREE)-enriched patterns ($La_{(n)}/Yb_{(n)}$ = 1.6–1.8), with modest Nb–Ta depletion relative to LREEs ($Nb_{(n)}/La_{(n)}$ = 1.2–1.4, Fig. 4a). They are geochemically similar to E-MORB and OIB. Gabbros also have flat to slightly LREE-fractionated patterns with $La_{(n)}/Yb_{(n)}$ = 0.7–1.5. Depletion in Nb is conspicuous ($Nb_{(n)}/La_{(n)}$ = 0.5–0.8). Granitic dikes are also enriched in LREE relative to heavy rare earth element (HREE) ($La_{(n)}/Yb_{(n)}$ = 1.8–3.3) and are depleted in Nb–Ta (e.g. $Nb_{(n)}/La_{(n)}$ = 0.4–0.8; Fig. 2a). SE Kamyaran lavas and dikes show flat to enriched LREE patterns ($La_{(n)}/Yb_{(n)}$ = 1.2–24.3), with or without Nb–Ta depletion ($Nb_{(n)}/La_{(n)}$ = 0.3–1).

Initial εNd ranges from + 6.5 to + 8.9 for Paleogene magmatic rocks from NW Kamyaran. Their $^{206}Pb/^{204}Pb$ and $^{208}Pb/^{204}Pb$ values change from 18.21 to 19.46 and 38.09 to 40.77, respectively. $^{207}Pb/^{204}Pb$ values range from 15.49 to 15.66. SE Kamyaran dikes and lavas have more variable εNd values; + 6.9 to – 5.3. Their $^{206}Pb/^{204}Pb$ and $^{208}Pb/^{204}Pb$ values vary from 18.54 to 18.86 and 38.58 to 39.19, respectively. All Paleogene rocks plot above the Northern Hemisphere Reference Line (NHRL) on the $^{207}Pb/^{204}Pb$ and $^{208}Pb/^{204}Pb$ v. $^{206}Pb/^{204}Pb$ diagram. SE Kamyaran magmatic rocks show higher involvement of sediments in their mantle source and/or contribution of Iranian continental crust – compared with the NW Kamyaran mafic rocks – although granites from NW Kamyaran have high Pb isotope ratios. The Pb isotopic composition of Paleogene samples lies between Zagros ophiolites and UDMB igneous rocks (Fig. 4c, d).

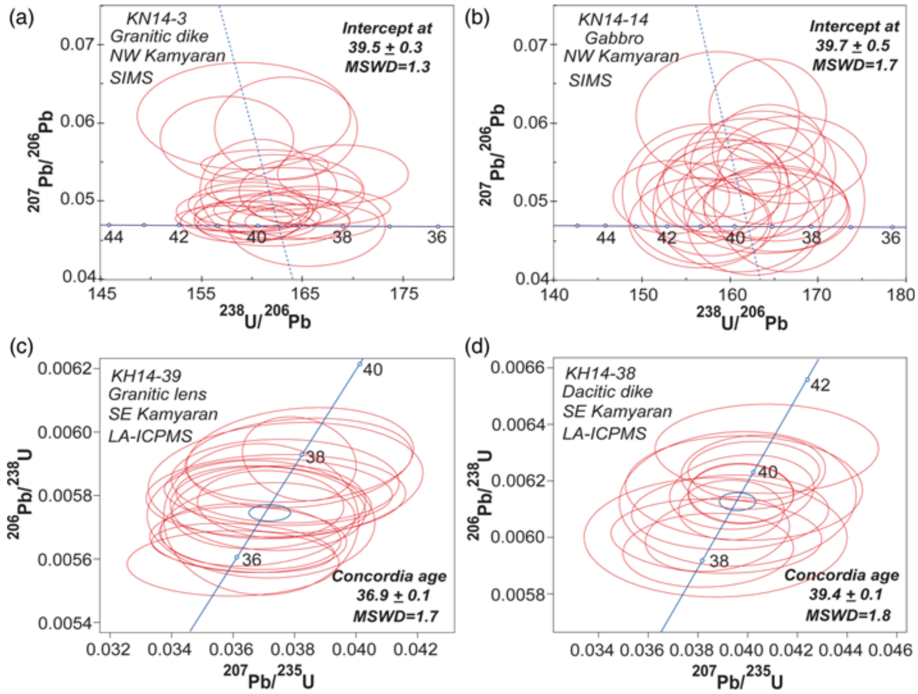


**Fig. 3.** Zircon LA-ICPMS and SIMS U–Pb plots for Paleogene magmatic rocks.

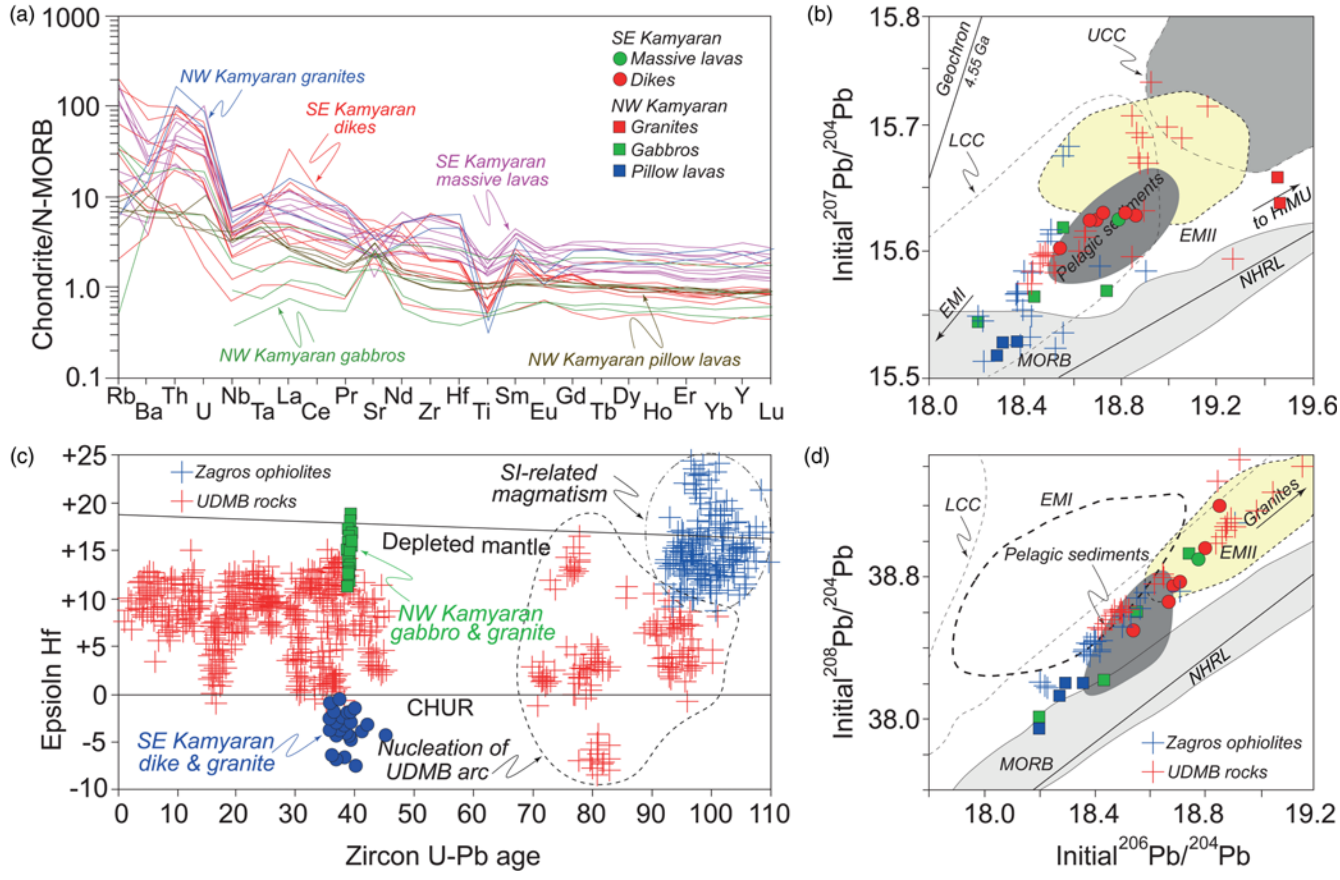


**Fig. 4.** (**a**) N-MORB normalized multi-elements patterns for analysed Paleogene igneous rocks. (**b**) Evolution plots of zircon Lu–Hf isotope composition of Paleogene rocks, Zagros ophiolites and UDMB-related rocks. CHUR = chondrite normalized uniform reservoir; depleted mantle array is based on data from modern Mid-Oceanic Ridge basalts with $^{176}$Hf/$^{177}$Hf = 0.28325 and using $^{176}$Lu/$^{177}$Hf = 0.0384 (Chauvel and Blichert-Toft 2001). Note that NW Kamyran igneous have more radiogenic Hf isotopic compositions than other Cenozoic igneous rocks from Iran. (**c**) $^{207}$Pb/$^{204}$Pb v. $^{206}$Pb/$^{204}$Pb and (**d**) $^{208}$Pb/$^{204}$Pb v. $^{206}$Pb/$^{204}$Pb for Paleogene magmatic rocks. The composition of the mantle components EM-1 and EM-2 are from Zindler and Hart (1986), whereas composition of subducted sediments is from Plank and Langmuir (1998). MORB and crust data are from Nowell *et al.* (1998); Pearce *et al.* (1999); Chauvel and Blichert-Toft (2001); Woodhead *et al.* (2001). NHRL is after Vervoort and Blichert-Toft (1999). Published zircon U–Pb–Hf and bulk rock data for UDMB and Zagros ophiolites are from Chiu *et al.* (2013); Moghadam *et al.* (2016); Chiu *et al.* (2017); Hosseini *et al.* (2017); Moghadam *et al.* (2017); Kazemi *et al.* (2019); Sepidbar *et al.* (2019).

## Discussion

Paleogene samples have MORB-like to arc-like geochemical signatures, which is shown by variable depletion in Nb–Ta and enrichment in large ion lithophile elements such as Th, U and Ba. In the Th/Yb v. Nb/Yb plot (Leat *et al.* 2004), pillow lavas and some massive lavas plot near the mantle array and are similar to MORBs. Dikes, gabbros and granitic dikes as well as most lavas show higher Th/Yb ratios and are similar to calc-alkaline rocks and arc tholeiites (Fig. 5a). In the field, MORB-like rocks seem to be younger than arc-related rocks. A plot of εNd(t) v. Sm/Nd (Fig. 5b) indicates that both depleted mantle similar to the source for normal-type Mid-Oceanic Ridge Basalts (N-MORB) and a variety of slab components similar to Izu-Bonin-Mariana (IBM) sediments and/or Cadomian continental crust of Iran were involved in magma genesis. SE Kamyaran dikes have less radiogenic Nd isotopes and lower Sm/Nd ratios compared with pillow lavas and gabbros. Samples with negative εNd(t) and εHf(t) values may reflect melting of a source with mixed proportions of sediment melts and depleted mantle-wedge materials, or contributions of continental crust.

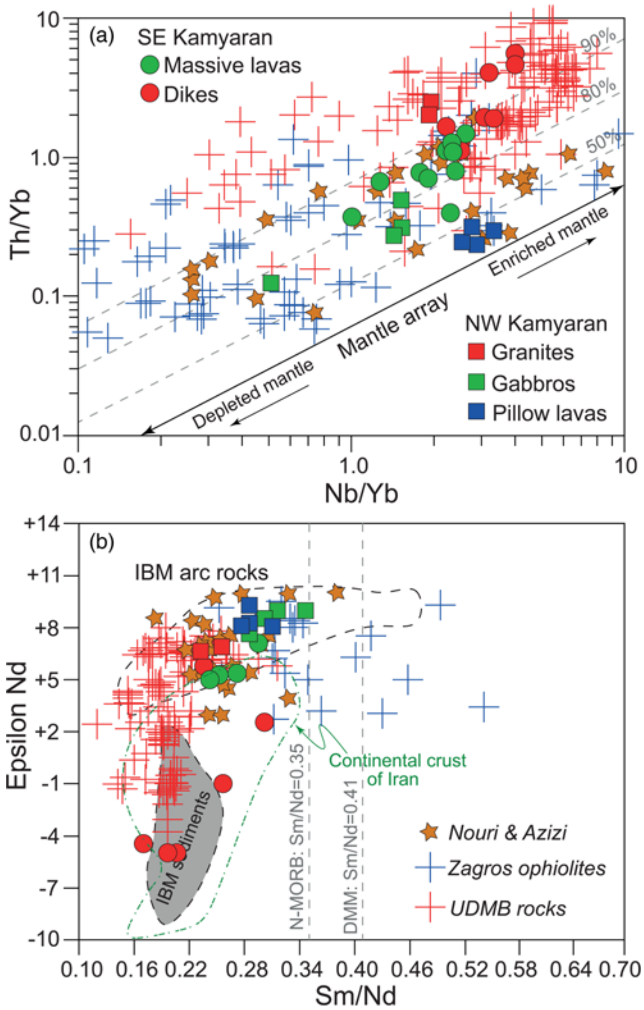


**Fig. 5.** (**a**) Th/Yb v. Nb/Yb plot for Paleogene rocks. Deviations above the mantle array are attributed to addition of subduction components or continental crust assimilation (dashed lines indicate the percent added) (Pearce *et al.* 1995). (**b**) εNd(t) v. Sm/Nd plot showing that most studied samples have sources that are more similar to Late Cretaceous ophiolites than UDMB igneous rocks. Data for IBM and pelagic sediments are from Yogodzinski *et al.* (2018). The composition of continental crust of Iran is from Moghadam *et al.* (2020*b*). For comparison, we also show the composition of Paleogene rocks from SE Kamyaran and Kermanshah (Azizi *et al.* 2011; Nouri *et al.* 2017).

Our new zircon U–Pb ages confirm Eocene ages for magmatic rocks from NW and SE Kamyaran and rule out the Permian–Triassic Gondwana rifting model to generate these rocks. Field evidence shows that Paleogene melts were injected into Late Cretaceous Zagros forearc ophiolites. Paleogene igneous rocks formed in a deep oceanic basin, represented by a thick pile (> 1000 m) of pillow lavas and interlayered pelagic siliceous sediments. NW Kamyaran preserves tilted, quasi-continuous exposures of oceanic crust where complementary lower and upper crust is exposed. No mantle rocks are exposed with these, and for this reason the Paleogene oceanic crust is not considered to be an ophiolite. It has been suggested that these rocks manifest a Paleogene intra-oceanic arc and back-arc (Ali *et al.* 2013; Whitechurch *et al.* 2013), but this is inconsistent with the observation that the Paleogene oceanic realm formed in a forearc setting. A complex scenario calling for an intra-oceanic arc with a back-arc basin to have coexisted with a continental arc on Iranian crust (the UDMB) – with two subduction systems operating at the same time – is unnecessarily complex. It is also geodynamically and geophysically inconsistent with seismic and mantle tomography data that are most consistent with a single, N-dipping subduction zone (e.g. Al-Lazki *et al.* 2004; Molinaro *et al.* 2005; Entezar-Saadat *et al.* 2017 and references therein).

Continental collision and slab break-off scenarios are more useful to explain the formation of Miocene UDMB adakitic magmas since there are several lines of evidence – including tectonics – that the collision between Iran and Arabia began *c.* 25 Ma, during the Late

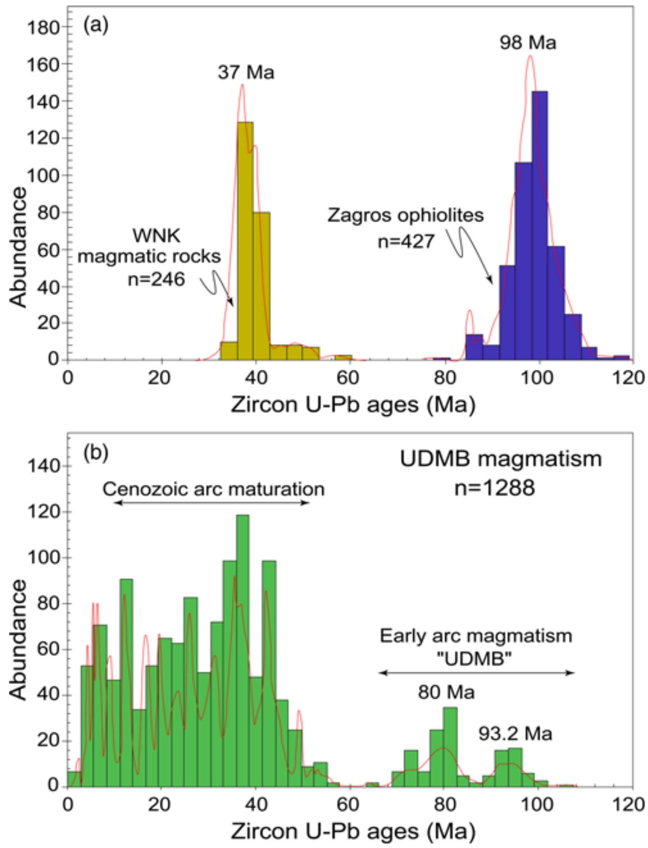


**Fig. 6.** Histograms showing the magmatic age distribution of (**a**) Walash–Naopurdan–Kamyran (WNK) series igneous rocks (-yellow) and Zagros Late Cretaceous ophiolites (-blue), and (**b**) UDMB magmatic rocks. Zagros ophiolites are as old as *c.* 110 Ma with a peak at *c.* 98 Ma (**a**). Magmatic rocks along the Iran–Iraq border show magmatic climax at *c.* 37, indistinguishable from the UDMB magmatic climax. Published zircon U–Pb data from Iran are from Chiu *et al.* (2013); Moghadam *et al.* (2016); Chiu *et al.* (2017); Hosseini *et al.* (2017); Moghadam *et al.* (2017); Kazemi *et al.* (2019); Sepidbar *et al.* (2019).

Oligocene McQuarrie and van Hinsbergen 2013; Barber *et al.* 2018). Apatite (U–Th)/He cooling ages of *c.* 20 Ma from core complex of central Iran further suggest an early Miocene period of north–south shortening related to Late Oligocene collision (Verdel *et al.* 2007). However, there is also evidence for initial collision between Arabia and Eurasia (including Iran) beginning *c.* 34 Ma (Allen and Armstrong 2008).

We agree that formation of the Paleogene oceanic realm along the Iran–Iraq border was related to a phase of hyperextension. Strong evidence for Paleogene extension is shown elsewhere in the UDMB, producing numerous arc-related extensional basins and core complexes in the upper plate of the Neotethyan subduction zone (Fig. 1a). Paleogene extension was also responsible for forming basins behind the UDMB with thick sequences of volcano-sedimentary rocks, such as those in N and NE Iran (Vincent *et al.* 2005; Verdel *et al.* 2011; Sepidbar *et al.* 2019). There is an age correlation between Paleogene magmatism along the Iran–Iraq border with a peak at *c.* 37 Ma and magmatism in UDMB which started at *c.* 50 Ma onwards (Fig. 6). These ages also overlap with those of magmatic rocks from back-arc basins in N and NE Iran (Moghadam *et al.* 2020*a*). Strong extension of Iran continental crust may also have caused Paleogene high-flux magmatism in the UDMB (Verdel *et al.* 2011; Moghadam *et al.* 2018; Sepidbar *et al.* 2019). One of these basins, including the WNK basin(s) along the Iraq–Iran border, rifted sufficiently to form new oceanic lithosphere.

Zircon Hf–O and bulk rock Nd isotope composition of some WNK igneous rocks show derivation from more depleted mantle (εHf(t) about + 15, εNd(t) about + 7, $\delta^{18}O$ about + 5.5) than that responsible for UDMB arc magmatism (εHf(t) about + 9, εNd(t) about + 3; $\delta^{18}O$ about + 6.5) (Fig. 7). These isotopic signatures are similar to those of Late Cretaceous Zagros ophiolites except for SE Kamyaran lavas and dikes which show probable involvement of Iran continental crust. Paleogene forearc rifting to form the WNK basin(s) could reflect weakening of the Iran forearc lithosphere due to slab-released fluids and melts (Baitsch-Ghirardello *et al.* 2014). This also explains the occurrence of older magmatic rocks (*c.* 40–39 Ma) with trace of extreme contribution of sediment melts and fluids (Fig. 5a). Resolving the subduction contribution for SE Kamyran magmas from trace elements is complicated by isotopic evidence that the edge of Iran Ediacaran–Early Neoproterozoic crust was involved in magma-genesis. Younger rocks (*c.* 36 Ma) with MORB-like signatures were likely generated due to decompression of upwelling mantle beneath the rift with minor contribution of slab-

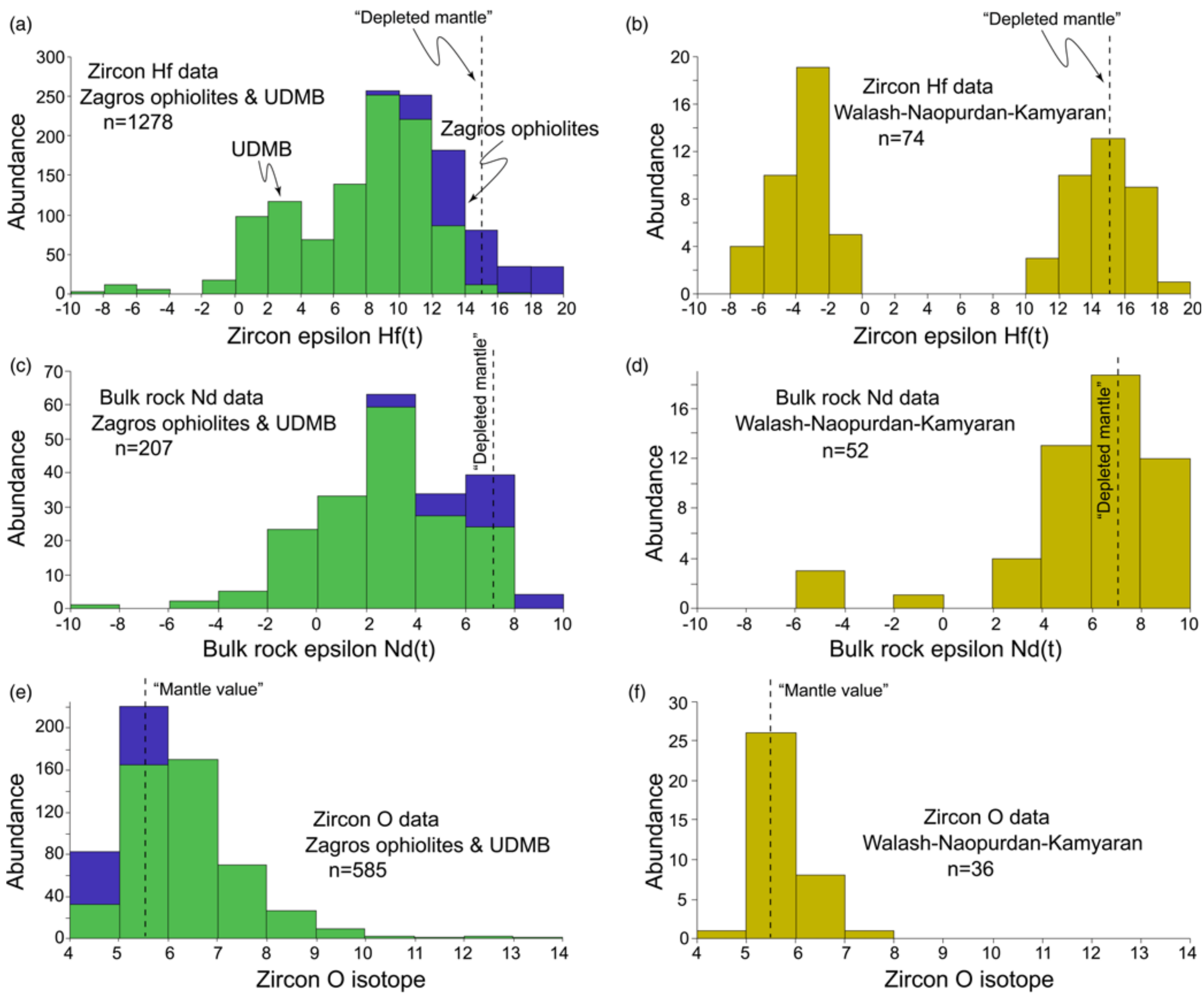


**Fig. 7.** Histograms showing zircon Hf–O and bulk rock Nd isotopic composition of magmatic rocks from Walash–Naopurdan–Kamyran (WNK) igneous rocks, Zagros ophiolites and UDMB magmatic rocks. UDMB rocks have evolved zircon Hf–O and bulk rock Nd isotopic signature than Paleogene rocks except some older magmatic rocks (*c.* 40–39 Ma) with trace of involvement of old continental crust of Iran. References for published zircon Hf–O and bulk rock Nd data for Zagros ophiolites and UDMB are similar to Figures 5 and 6.

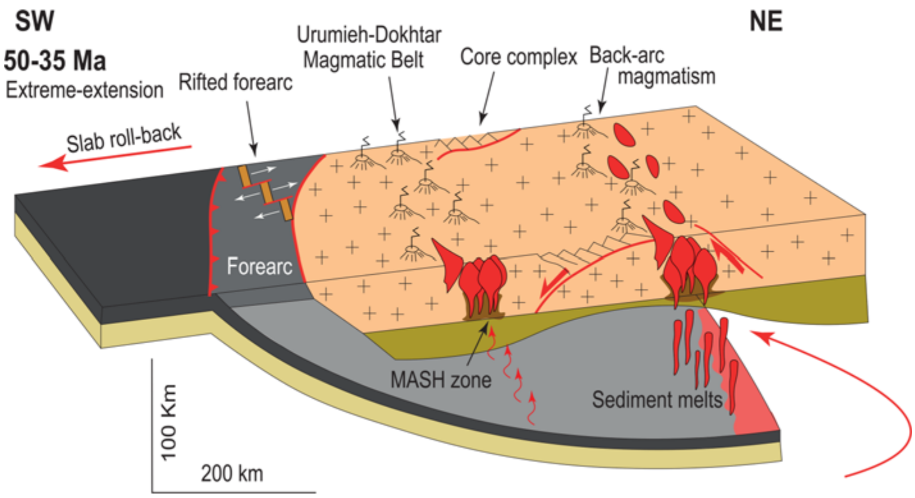


**Fig. 8.** Simplified cross-section of the Paleogene convergent margin of Iran, emphasizing extreme extension in the Iranian plateau during Paleogene (50–35 Ma). This figure also indicates the positions of the forearc rift, Urumieh–Dokhtar Magmatic Belt (UDMB), back-arc magmatism and core complex. Small wavy red lines show the trajectory of slab fluids whereas continuous red line shows the asthenosphere mantle flow.

derived fluids, arguing against an important role for hydrous weakening of the lithosphere. Regardless, the forearc rifting scenario we prefer is similar to that documented for the SE Mariana forearc rift, where the Izu–Bonin–Mariana convergent margin experienced forearc rifting *c.* 2 Ma years ago (Ribeiro *et al.* 2013). In the SE Mariana forearc rift strong regional extension caused MORB-type melts to disrupt Eocene boninitic and arc tholeiitic crust. This evolution is very similar to that of the Zagros Paleogene forearc rift. There are two significant differences: (1) in Iran continental crust was involved whereas Mariana rifting only involved oceanic lithosphere; and (2) the Mariana forearc rift cut across the forearc perpendicular to the trench whereas the Iran forearc rift was parallel to forearc and trench.

Traces of other Paleogene oceanic basin(s) may exist elsewhere to the SE in Iran and/or towards the NW, in SE Turkey, wherever the Late Cretaceous forearc suffered extreme extension during the Paleogene. Further studies are needed to understand the age and geochemistry of such sequences; e.g., in the Neyriz ophiolite where younger volcanic rocks and sediments known as the Hassan–Abad complex are present (Babaie *et al.* 2001).

## Conclusions

Paleogene magmatic rocks including gabbros, granites, dikes and overlying pillow lavas are present in the Iran–Iraq border region, in a > 220 km-long belt from SE of Kermanshah (Iran) to Hasanbag (Iraq). These igneous rocks are accompanied by and/or interlayered with Paleogene sandstones and pelagic limestones. Field observations indicate that Paleogene rocks were injected into and/or underlain by Late Cretaceous Zagros forearc ophiolites, the Kurdistan–Kermanshah ophiolites. Paleogene igneous rocks show MORB- to arc-like geochemical signatures. Zircon U–Pb results show crystallization ages of *c.* 40–37 Ma for these rocks. We believe that a phase of Paleogene hyperextension in the Iranian Plateau – the main triggers for core complex exhumation and high-flux magmatism in the UDMB – was also responsible for forming the Paleogene forearc rift that is now preserved along the Iran–Iraq border.

**Acknowledgements** This study was funded by the 'National Key Research and Development Program of China (2016YFE0203000)' and by 'Chinese Academy of Sciences, President's International Fellowship Initiative (PIFI, 2019VCB0013)'. We are very grateful to Mark Allen and two anonymous reviewers for their constructive reviews of the manuscript. Editorial suggestions by Tyrone Rooney are also appreciated. We are also very grateful to Y. Liu, X.X. Ling, J. Li, G. Tang, Y.H. Yang, X. Yan and D. Zhang (IGG-CAS) for their assistance during zircon SIMS and LA-ICPMS dating and O isotope, LA-MC-ICPMS Lu–Hf isotope and SEM analyses. All logistical support for the field work came from Damghan University, Iran. This is UTD Geosciences contribution # 1362.

**Funding** This work funded by the National Key Research and Development Program of China (2016YFE0203000) to QL and by Chinese Academy of Sciences, President's International Fellowship Initiative (PIFI, 2019VCB0013) to HSM.

**Author contributions** **HSM**: conceptualization (lead), formal analysis (lead), investigation (lead), writing – original draft (lead); **QL**: data curation (equal), funding acquisition (equal); **RJS**: writing – review & editing (equal); **MC**: formal analysis (equal); **OK**: review and editing (equal); **BR**: investigation (equal).

**Data availability statement** All data generated or analysed during this study are included in this published article (and its supplementary information files).

*Scientific editing by Tyrone Rooney*

## References

Agard, P., Omrani, J., Jolivet, L. and Mouthereau, F. 2005. Convergence history across Zagros (Iran): constraints from collisional and earlier deformation. *International Journal of Earth Sciences*, **94**, 401–419, https://doi.org/10.1007/s00531-005-0481-4

Ali, S.A., Buckman, S., Aswad, K.J., Jones, B.G., Ismail, S.A. and Nutman, A.P. 2013. The tectonic evolution of a Neo-Tethyan (Eocene–Oligocene) island-arc (Walash and Naopurdan groups) in the Kurdistan region of the Northeast Iraqi Zagros Suture Zone. *Island Arc*, **22**, 104–125, https://doi.org/10.1111/iar.12007

Al-Lazki, A.I., Sandvol, E., Seber, D., Barazangi, M., Turkelli, N. and Mohamad, R. 2004. Pn tomographic imaging of mantle lid velocity and anisotropy at the junction of the Arabian, Eurasian and African plates. *Geophysical Journal International*, **158**, 1024–1040. https://doi.org/10.1111/j.1365-246X.2004.02355.x

Allen, M.B. and Armstrong, H.A. 2008. Arabia–Eurasia collision and the forcing of mid-Cenozoic global cooling. *Palaeogeography, Palaeoclimatology, Palaeoecology*, **265**, 52–58, https://doi.org/10.1016/j.palaeo.2008.04.021

Ao, S., Xiao, W. *et al.* 2016. U–Pb zircon ages, field geology and geochemistry of the Kermanshah ophiolite (Iran): from continental rifting at 79 Ma to oceanic core complex at ca. 36 Ma in the southern Neo-Tethys. *Gondwana Research*, **31**, 305–318, https://doi.org/10.1016/j.gr.2015.01.014

Aswad, K.J. 1999. Arc-continent collision in Northeastern Iraq as evidenced by Mawat and Penjwin Ophiolite Complexes. *Raffidain Journal of Science*, **10**, 51–61.

Aswad, K.J., Aziz, N.R. and Koyi, H.A. 2011. Cr-spinel compositions in serpentinites and their implications for the petrotectonic history of the Zagros Suture Zone, Kurdistan Region, Iraq. *Geological Magazine*, **148**, 802–818, https://doi.org/10.1017/S0016756811000422

Aswad, K.J.A., Al-Samman, A.H.M., Aziz, N.R.H. and Koyi, A.M.A. 2014. The geochronology and petrogenesis of Walash volcanic rocks, Mawat nappes: constraints on the evolution of the northwestern Zagros suture zone, Kurdistan Region, Iraq. *Arabian Journal of Geosciences*, **7**, 1403–1432, https://doi.org/10.1007/s12517-013-0873-x

Aziz, N.R., Elias, E.M. and Aswad, K.J.A. 2011*a*. Rb–Sr and Sm–Nd isotope study of serpentinites and their impact on the tectonic setting of Zagros Suture Zone, NE-Iraq. *Iraqi Bulletin of Geology and Mining*, **7**, 67–75.

Aziz, N.R.H., Aswad, K.J.A. and Koyi, H.A. 2011*b*. Contrasting settings of serpentinite bodies in the northwestern Zagros Suture Zone, Kurdistan Region, Iraq. *Geological Magazine*, **148**, 819–837, https://doi.org/10.1017/S0016756811000409

Azizi, H., Tanaka, T., Asahara, Y., Chung, S.L. and Zarrinkoub, M.H. 2011. Discrimination of the age and tectonic setting for magmatic rocks along the Zagros thrust zone, northwest Iran, using the zircon U–Pb age and Sr–Nd isotopes. *Journal of Geodynamics*, **52**, 304–320. https://doi.org/10.1016/j.jog.2011.03.001

Babaie, H.A., Ghazi, A.M., Babaei, A., La Tour, T.E. and Hassanipak, A.A. 2001. Geochemistry of arc volcanic rocks of the Zagros Crush Zone, Neyriz, Iran. *Journal of Asian Earth Sciences*, **19**, 61–76, https://doi.org/10.1016/S1367-9120(00)00012-2

Babaei, A., Babaie, H.A. and Arvin, M. 2005. Tectonic evolution of the Neyriz ophiolite, Iran: an accretionary prism model. *Ofioliti*, **30**, 65–74.

Babaie, H.A., Babaei, A., Ghazi, A.M. and Arvin, M. 2006. Geochemical, Ar-40/Ar-39 age, and isotopic data for crustal rocks of the Neyriz ophiolite, Iran. *Canadian Journal of Earth Sciences*, **43**, 57–70, https://doi.org/10.1139/e05-111

Baitsch-Ghirardello, B., Gerya, T.V. and Burg, J.-P. 2014. Geodynamic regimes of intra-oceanic subduction: implications for arc extension vs. shortening processes. *Gondwana Research*, **25**, 546–560, https://doi.org/10.1016/j.gr.2012.11.003

Barber, D.E., Stockli, D.F., Horton, B.K. and Koshnaw, R.I. 2018. Cenozoic exhumation and foreland basin evolution of the Zagros orogen during the Arabia–Eurasia collision, Western Iran. *Tectonics*, **37**, 4396–4420. https://doi.org/10.1029/2018TC005328

Chauvel, C. and Blichert-Toft, J. 2001. A hafnium isotope and trace element perspective on melting of the depleted mantle. *Earth and Planetary Science Letters*, **190**, 137–151, https://doi.org/10.1016/S0012-821X(01)00379-X

Chauvet, F., Lapierre, H. *et al.* 2011. Triassic alkaline magmatism of the Hawasina Nappes: post-breakup melting of the Oman lithospheric mantle modified by the Permian Neotethyan Plume. *Lithos*, **122**, 122–136, https://doi.org/10.1016/j.lithos.2010.12.006

Chiu, H.Y., Chung, S.L., Zarrinkoub, M.H., Mohammadi, S.S., Khatib, M.M. and Iizuka, Y. 2013. Zircon U-Pb age constraints from Iran on the magmatic evolution related to Neotethyan subduction and Zagros orogeny. *Lithos*, **162**, 70–87. https://doi.org/10.1016/j.lithos.2013.01.006

Chiu, H.Y., Chung, S.L. *et al.* 2017. Zircon Hf isotopic constraints on magmatic and tectonic evolution in Iran: implications for crustal growth in the Tethyan orogenic belt. *Journal of Asian Earth Sciences*, **145**, 652–669. https://doi.org/10.1016/j.jseaes.2017.06.011

Dilek, Y. and Altunkaynak, S. 2010. Geochemistry of Neogene-Quaternary alkaline volcanism in western Anatolia, Turkey, and implications for the Aegean mantle. *International Geology Review*, **52**, 631–655, https://doi.org/10.1080/00206810903495020

Dilek, Y. and Thy, P. 2009. Island arc tholeiite to boninitic melt evolution of the Cretaceous Kizildag (Turkey) ophiolite: model for multi-stage early arc-forearc magmatism in Tethyan subduction factories. *Lithos*, **113**, 68–87, https://doi.org/10.1016/j.lithos.2009.05.044

Dilek, Y., Furnes, H. and Shallo, M. 2007. Suprasubduction zone ophiolite formation along the periphery of Mesozoic Gondwana. *Gondwana Research*, **11**, 453–475. https://doi.org/10.1016/j.gr.2007.01.005

Dilek, Y., Imamverdiyev, N. and Altunkaynak, S. 2010. Geochemistry and tectonics of Cenozoic volcanism in the Lesser Caucasus (Azerbaijan) and the peri-Arabian region: collision-induced mantle dynamics and its magmatic fingerprint. *International Geology Review*, **52**, 536–578. https://doi.org/10.1080/00206810903360422

Entezar-Saadat, V., Motavalli-Anbaran, S.-H. and Zeyen, H. 2017. Lithospheric structure of the Eastern Iranian plateau from integrated geophysical modeling: a transect from Makran to the Turan platform. *Journal of Asian Earth Sciences*, **138**, 357–366. https://doi.org/10.1016/j.jseaes.2017.02.024

Ghazi, J.M., Moazzen, M., Rahgoshay, M. and Moghadam, H.S. 2010. Mineral chemical composition and geodynamic significance of peridotites from Nain ophiolite, central Iran. *Journal of Geodynamics*, **49**, 261–270, https://doi.org/10.1016/j.jog.2010.01.004

Golonka, J. 2004. Plate tectonic evolution of the southern margin of Eurasia in the Mesozoic and Cenozoic. *Tectonophysics*, **381**, 235–273. https://doi.org/10.1016/j.tecto.2002.06.004

Hassan, M.M., Jones, B.G., Buckman, S., Al Jubory, A.I. and Ismail, S.A. 2015. Source area and tectonic provenance of Paleocene–Eocene red bed clastics from the Kurdistan area NE Iraq: bulk-rock geochemistry constraints. *Journal of African Earth Sciences*, **109**, 68–86, https://doi.org/10.1016/j.jafrearsci.2015.04.019

Hosseini, M.R., Hassanzadeh, J., Alirezaei, S., Sun, W.D. and Li, C.Y. 2017. Age revision of the Neotethyan arc migration into the southeast Urumieh-Dokhtar belt of Iran: geochemistry and U-Pb zircon geochronology. *Lithos*, **284**, 296–309. https://doi.org/10.1016/j.lithos.2017.03.012

Ishizuka, O., Tani, K. and Reagan, M.K. 2014. Izu-Bonin-Mariana forearc crust as a modern ophiolite analogue. *Elements*, **10**, 115–120. https://doi.org/10.2113/gselements.10.2.115

Kazemi, Z., Ghasemi, H., Tilhac, R., Griffin, W., Moghadam, H.S., O'Reilly, S. and Mousivand, F. 2019. Late Cretaceous subduction-related magmatism on the southern edge of Sabzevar basin, NE Iran. *Journal of the Geological Society*, **176**, 530–552. https://doi.org/10.1144/jgs2018-076

Leat, P.T., Pearce, J.A., Barker, P.F., Millar, I.L., Barry, T.L. and Larter, R.D. 2004. Magma genesis and mantle flow at a subducting slab edge: the South Sandwich arc-basin system. *Earth and Planetary Science Letters*, **227**, 17–35. https://doi.org/10.1016/j.epsl.2004.08.016

Mazhari, S.A., Bea, F. *et al.* 2009. The Eocene bimodal Piranshahr massif of the Sanandaj–Sirjan Zone, NW Iran: a marker of the end of the collision in the Zagros orogen. *Journal of the Geological Society*, **166**, 53–69. https://doi.org/10.1144/0016-76492008-022

McQuarrie, N. and van Hinsbergen, D.J.J. 2013. Retrodeforming the Arabia-Eurasia collision zone: age of collision versus magnitude of continental subduction. *Geology*, **41**, 315–318, https://doi.org/10.1130/G33591.1

Moghadam, H.S. and Stern, R.J. 2011. Geodynamic evolution of Upper Cretaceous Zagros ophiolites: formation of oceanic lithosphere above a nascent subduction zone. *Geological Magazine*, **148**, 762–801, https://doi.org/10.1017/S0016756811000410

Moghadam, H.S. and Stern, R.J. 2015. Ophiolites of Iran: keys to understanding the tectonic evolution of SW Asia: (II) Mesozoic ophiolites. *Journal of Asian Earth Sciences*, **100**, 31–59. https://doi.org/10.1016/j.jseaes.2014.12.016

Moghadam, H.S., Stern, R.J. and Rahgoshay, M. 2010. The Dehshir ophiolite (central Iran): geochemical constraints on the origin and evolution of the Inner Zagros ophiolite belt. *Geological Society of America Bulletin*, **122**, 1516–1547. https://doi.org/10.1130/B30066.1

Moghadam, H.S., Stern, R.J., Kimura, J.I., Hirahara, Y., Senda, R. and Miyazaki, T. 2012. Hf-Nd isotope constraints on the origin of Dehshir Ophiolite, Central Iran. *Island Arc*, **21**, 202–214, https://doi.org/10.1111/j.1440-1738.2012.00815.x

Moghadam, H.S., Mosaddegh, H. and Santosh, M. 2013*a*. Geochemistry and petrogenesis of the Late Cretaceous Haji-Abad ophiolite (Outer Zagros Ophiolite Belt, Iran): implications for geodynamics of the Bitlis-Zagros suture zone. *Geological Journal*, **48**, 579–602. https://doi.org/10.1002/gj.2458

Moghadam, H.S., Stern, R.J., Chiaradia, M. and Rahgoshay, M. 2013*b*. Geochemistry and tectonic evolution of the Late Cretaceous Gogher-Baft ophiolite, central Iran. *Lithos*, **168**, 33–47. https://doi.org/10.1016/j.lithos.2013.01.013

Moghadam, H.S., Khedr, M.Z. *et al.* 2014. Supra-subduction zone magmatism of the Neyriz ophiolite, Iran: constraints from geochemistry and Sr-Nd-Pb isotopes. *International Geology Review*, **56**, 1395–1412. https://doi.org/10.1080/00206814.2014.942391

Moghadam, H.S., Rossetti, F. *et al.* 2016. The calc-alkaline and adakitic volcanism of the Sabzevar structural zone (NE Iran): implications for the Eocene magmatic flare-up in Central Iran. *Lithos*, **248**, 517–535. https://doi.org/10.1016/j.lithos.2016.01.019

Moghadam, H.S., Griffin, W.L. *et al.* 2017. Crustal evolution of NW Iran: Cadomian arcs, archean fragments and the Cenozoic magmatic flare-up. *Journal of Petrology*, **58**, 2143–2190. https://doi.org/10.1093/petrology/egy005

Moghadam, H.S., Griffin, W.L. *et al.* 2018. Roll-back, extension and mantle upwelling triggered Eocene potassic magmatism in NW Iran. *Journal of Petrology*, **59**, 1417–1465. https://doi.org/10.1093/petrology/egy067

Moghadam, H.S., Li, Q.L. *et al.* 2020*a*. Neotethyan subduction ignited the Iran arc and backarc differently. *Journal of Geophysical Research (Solid Earth)*, **125**, e2019JB018460, https://doi.org/10.1029/2019JB018460

Moghadam, H.S., Li, Q.L. *et al.* 2020*b*. Repeated magmatic buildup and deep 'hot zones' in continental evolution: the Cadomian crust of Iran. *Earth and Planetary Science Letters*, 531, 115989, https://doi.org/10.1016/j.epsl.2019.115989

Molinaro, M., Zeyen, H. and Laurencin, X. 2005. Lithospheric structure beneath the south-eastern Zagros Mountains, Iran: recent slab break-off? *Terra Nova*, **17**, 1–6. https://doi.org/10.1111/j.1365-3121.2004.00575.x

Monsef, I., Monsef, R. *et al.* 2018. Evidence for an early-MORB to fore-arc evolution within the Zagros suture zone: constraints from zircon U-Pb geochronology and geochemistry of the Neyriz ophiolite (South Iran). *Gondwana Research*, **62**, 287–305. https://doi.org/10.1016/j.gr.2018.03.002

Nouri, F., Azizi, H. *et al.* 2016. Age and petrogenesis of Na-rich felsic rocks in western Iran: evidence for closure of the southern branch of the Neo-Tethys in the Late Cretaceous. *Tectonophysics*, **671**, 151–172. https://doi.org/10.1016/j.tecto.2015.12.014

Nouri, F., Asahara, Y., Azizi, H., Yamamoto, K. and Tsuboi, M. 2017. Geochemistry and petrogenesis of the Eocene-back arc mafic rocks in the Zagros suture zone, northern Noorabad, western Iran. *Chemie Der Erde-Geochemistry*, **77**, 517–533. https://doi.org/10.1016/j.chemer.2017.06.002

Nowell, G., Kempton, P., Noble, S., Fitton, J., Saunders, A., Mahoney, J. and Taylor, R. 1998. High precision Hf isotope measurements of MORB and OIB by thermal ionisation mass spectrometry: insights into the depleted mantle. *Chemical Geology*, **149**, 211–233, https://doi.org/10.1016/S0009-2541(98)00036-9

Numan, N.M. 2001. Cretaceous and Tertiary Alpine subductional history in Northern Iraq. *Iraqi J Earth Sci*, **1**, 59–74.

Pearce, J.A., Baker, P.E., Harvey, P.K. and Luff, I.W. 1995. Geochemical evidence for subduction fluxes, mantle melting and fractional crystallization

beneath the South Sandwich-Island Arc. *Journal of Petrology*, **36**, 1073–1109, https://doi.org/10.1093/petrology/36.4.1073
Pearce, J., Kempton, P., Nowell, G. and Noble, S. 1999. Hf-Nd element and isotope perspective on the nature and provenance of mantle and subduction components in Western Pacific arc-basin systems. *Journal of Petrology*, **40**, 1579–1611, https://doi.org/10.1093/petroj/40.11.1579
Plank, T. and Langmuir, C.H. 1998. The chemical composition of subducting sediment and its consequences for the crust and mantle. *Chemical Geology*, **145**, 325–394, https://doi.org/10.1016/S0009-2541(97)00150-2
Ribeiro, J.M., Stern, R.J. *et al.* 2013. Geodynamic evolution of a forearc rift in the southernmost Mariana Arc. *Island Arc*, **22**, 453–476, https://doi.org/10.1111/iar.12039
Saccani, E., Allahyari, K. and Rahimzadeh, B. 2014. Petrology and geochemistry of mafic magmatic rocks from the Sarve-Abad ophiolites (Kurdistan region. Iran): evidence for interaction between MORB-type asthenosphere and OIB-type components in the southern Neo-Tethys Ocean. *Tectonophysics*, **621**, 132–147, https://doi.org/10.1016/j.tecto.2014.02.011
Sepidbar, F., Shafaii Moghadam, H., Zhang, L., Li, J.-W., Ma, J., Stern, R.J. and Lin, C. 2019. Across-arc geochemical variations in the Paleogene magmatic belt of Iran. *Lithos*, **344-345**, 280–296. https://doi.org/10.1016/j.lithos.2019.06.022
van Hinsbergen, D.J., Maffione, M., Koornneef, L.M. and Guilmette, C. 2019. Kinematic and paleomagnetic restoration of the Semail ophiolite (Oman) reveals subduction initiation along an ancient Neotethyan fracture zone. *Earth and Planetary Science Letters*, **518**, 183–196, https://doi.org/10.1016/j.epsl.2019.04.038
Verdel, C., Wernicke, B.P., Ramezani, J., Hassanzadeh, J., Renne, P.R. and Spell, T.L. 2007. Geology and thermochronology of Tertiary Cordilleran-style metamorphic core complexes in the Saghand region of central Iran. *Geological Society of America Bulletin*, **119**, 961–977. https://doi.org/10.1130/B26102.1
Verdel, C., Wernicke, B.P., Hassanzadeh, J. and Guest, B. 2011. A Paleogene extensional arc flare-up in Iran. *Tectonics*, **30**, https://doi.org/10.1029/2010TC002809
Vervoort, J.D. and Blichert-Toft, J. 1999. Evolution of the depleted mantle: Hf isotope evidence from juvenile rocks through time. *Geochimica Et Cosmochimica Acta*, **63**, 533–556, https://doi.org/10.1016/S0016-7037(98)00274-9
Vincent, S.J., Allen, M.B., Ismail-Zadeh, A.D., Flecker, R., Foland, K.A. and Simmons, M.D. 2005. Insights from the Talysh of Azerbaijan into the Paleogene evolution of the South Caspian region. *Geological Society of America Bulletin*, **117**, 1513–1533, https://doi.org/10.1130/B25690.1
Whitechurch, H., Omrani, J., Agard, P., Humbert, F., Montigny, R. and Jolivet, L. 2013. Evidence for Paleocene–Eocene evolution of the foot of the Eurasian margin (Kermanshah ophiolite, SW Iran) from back-arc to arc: implications for regional geodynamics and obduction. *Lithos*, **182–183**, 11–32. https://doi.org/10.1016/j.lithos.2013.07.017
Woodhead, J., Hergt, J., Davidson, J. and Eggins, S. 2001. Hafnium isotope evidence for 'conservative' element mobility during subduction zone processes. *Earth and Planetary Science Letters*, **192**, 331–346, https://doi.org/10.1016/S0012-821X(01)00453-8
Yogodzinski, G.M., Bizimis, M. *et al.* 2018. Implications of Eocene-age Philippine Sea and forearc basalts for initiation and early history of the Izu-Bonin-Mariana arc. *Geochimica Et Cosmochimica Acta*, **228**, 136–156. https://doi.org/10.1016/j.gca.2018.02.047
Zindler, A. and Hart, S. 1986. Chemical geodynamics. *Annual Review of Earth and Planetary Sciences*, **14**, 493–571, https://doi.org/10.1146/annurev.ea.14.050186.002425